Oxygen isotope effect on the vibrational modes of La$_{1-x}$Ca$_x$MnO$_3$

J. C. Irwin and J. Chrzanowski

Department of Physics, Simon Fraser University, Burnaby, British Columbia, Canada V5A 1S6

J. P. Franck

Department of Physics, University of Alberta, Edmonton, Alberta, Canada T6G 2J1

(Received 8 June 1998; revised manuscript received 4 September 1998)

Raman-scattering experiments have been carried out on polycrystalline samples of La$_{0.65}$Ca$_{0.35}$Mn ^{16}O$_3$ and isotope-exchanged La$_{0.65}$Ca$_{0.35}$Mn ^{18}O$_3$ as a function of temperature. The most interesting feature in the spectra is a vibrational mode that occurs at a nominal frequency of $\omega_0 \approx 230$ cm^{-1}, which is assigned to an out-of-phase rotational mode that involves motion of the O(1) atoms. The frequency of this phonon depends strongly on the Ca concentration and has been correlated with the strength of the Jahn-Teller lattice distortion as measured by the tolerance factor. As the temperature is lowered through the critical temperature, the phonon frequency ω_0 increases rather abruptly and continues to harden as the temperature is lowered further. In contrast, the linewidth Γ_0 decreases abruptly when the sample passes through the transition from the paramagnetic insulating phase to the more metallic ferromagnetic phase. The observed temperature dependences of the frequency and linewidth are well described by a model that incorporates a double-exchange mechanism in the presence of an electron-phonon interaction. The agreement between experiment and theory suggests that the temperature dependence of the phonon is determined primarily by the spin alignment associated with the double-exchange mechanism. The results for both ω_0 and Γ_0 imply that there are no significant structural modifications associated with the transition to the ferromagnetic phase. Finally, the linewidth Γ_0 in the isotope-exchanged sample (^{18}O) is smaller than in the ^{16}O sample, an observation that is consistent with the smaller electron-phonon-coupling constant in the ^{18}O compound. [S0163-1829(99)06413-9]

I. INTRODUCTION

It has been known for some time that the mixed-valence compounds La$_{1-x}$Ca$_x$Mn$_{1-x}^{3+}$Mn$_x^{4+}$O$_3$ (LCMO, $0 \leq x \leq 1$), have very interesting magnetic and electronic properties,[1-6] which are surprisingly sensitive[7] to the doping level x. For example, the end materials are both antiferromagnetic insulators for all $T < 150$ K and become paramagnetic insulators (PI's) at higher temperatures. However, when samples with Ca concentrations in the range $0.2 < x < 0.4$ are cooled to low temperatures, the high-temperature paramagnetic phase converts to a more metallic ferromagnetic (FM) state at the Curie temperature T_C. This approximate insulating-to-metallic transition is field dependent,[3] and recent attention has focused on the very large (''colossal'') magnetoresistance (CMR) that is observed[8] for temperatures near T_C.

The transition from the PI or magnetically disordered state to the more ordered FM metallic phase at lower temperatures was initially explained[4] in terms of a double-exchange mechanism. In this model two carriers hop simultaneously, one from a Mn^{3+} ion to an adjacent O^{2-} site and the other from the O^{2-} to a neighboring Mn^{4+}. This mechanism appeared to explain both the enhanced conductivity and, because of the large intra-atom exchange, the lower energy associated with the ferromagnetic state, although it was recognized[6] that the neglect of the electron-lattice coupling was a serious omission. This omission was reviewed more critically by Millis *et al.*[9] who found that the double-exchange model could not, by itself, explain the low critical temperature[9] and large magnetoresistance[8] in these materials.

They concluded that an additional mechanism was required and suggested[9-12] that a strong electron-phonon interaction arising from the Jahn-Teller (JT) splitting of the Mn^{3+} ion should be incorporated into the model. The resulting lattice distortion is thought to be large in the magnetically disordered regime above T_c, but should decrease[9,10] significantly on transition to the low-temperature magnetically ordered phase. Direct support for this suggestion has come from experiments involving local probes,[12-18] which have found that the MnO$_6$ octahedra are highly distorted for $T > T_c$ and that the magnitude of the distortion decreases with decreasing temperature near T_c.

The presence of strong electron-phonon interactions, or JT effects, in the insulating phase of the CMR compounds should be associated[9-11] with polaron formation, and a number of experiments[19-22] have produced supportive evidence in this regard. The observation[23-25] of large oxygen isotope shifts in the Curie temperature also emphasized[26] the importance of electron-phonon interactions in CMR compounds. The precise nature of this coupling, its relative importance, and the origin of the large isotope effect itself are not well understood. To gain insight into these aspects, and into other features such as charge ordering,[25] additional experiments on isotope-exchanged samples are required. In particular, it would appear that studies of the vibrational spectra of isotope-exchanged samples should provide important and interesting information.

Although optical studies are well suited for investigations of the interplay between the electronic, magnetic, and vibrational degrees of freedom in CMR compounds, relatively few such investigations[22,27-32] have been carried out to date.

In particular, Raman studies of the vibrational spectrum would appear to be warranted given that the temperature dependence of the vibrational spectrum should provide important information on structural changes associated with the transition to the low-temperature FM phase. The temperature dependence of the phonon frequencies and linewidths should also yield indirect information on the relative importance of the various interactions in determining the properties of the linear combination of molecular orbits (LCMO) at various temperatures. In this regard Iliev *et al.*[27,28] have carried out careful studies on single crystals of the undoped parent compound LaMnO$_3$ (LMO) and structurally related perovskites which have led to the symmetry identification of the important modes. The dependence of the Raman spectrum on Sr concentration in the CMR compound La$_{1-x}$Sr$_x$MnO$_3$ (LSMO) has been studied by Podobedev *et al.*[29] Since the properties of LSMO are very similar to those of LCMO, we expect the trends identified in their work[29] to also be relevant to LCMO. Gupta *et al.*[30] have also carried out a Raman investigation of LSMO. They found that the vibrational spectrum was very weak, and focused on the frequency and temperature dependence of a broad, high-energy peak centered near 2600 cm^{-1}. Although the origin of this peak was not determined definitively, it was attributed to scattering from electronic excitations. The weakness of the vibrational spectrum is consistent with the fact that the parent structure is a cubic perovskite which does not have any Raman-allowed vibrational modes.

We have carried out Raman experiments on LCMO ($x = 0.35$) compounds grown with the ^{16}O isotope and also on ^{18}O-exchanged samples. The observed vibrational spectra are similar in appearance and strength to those obtained[27,28] from LMO. Here we assume that the observed Raman modes, which are relatively weak, become Raman allowed because of the orthorhombic distortions that are present in both the LCMO and LMO structures. The frequency ω_0 (nominally 230 cm^{-1}) and linewidth Γ_0 of one of the modes are found to be sensitive to the transition at T_c and to the variation of temperature below T_c. It thus arises from the vibrations of atoms whose structural locations are affected by the transition. The observed variation of the frequency of this phonon with doping is correlated with the structural distortion of the lattice using the tolerance factor. The temperature dependences of both ω_0 and Γ_0 are compared to the predictions of a model by Lee and Min[33] that combines the double-exchange mechanism with an electron-phonon interaction. The experimental results are in good agreement with the predictions of this model, which suggests that the temperature dependence is primarily determined by changes in the ''double-exchange'' bandwidth. However, there is no evidence at any temperature of a Fano-type line shape that would imply a coupling[34] of the phonons with a metallic-type electronic continuum.

II. MATERIALS

A. Preparation

Samples of LCMO ($x = 0.35$) were prepared from stoichiometric mixtures of La$_2$O$_3$, CaCO$_3$, and MnO$_2$. The mixtures were fired in air at 1100 and 1200 °C repeatedly, with regrinding between firings. A dense pellet was obtained after
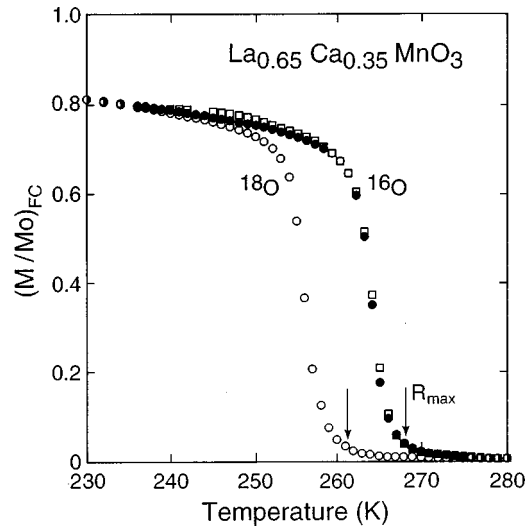

FIG. 1. Magnetization curves for pressed sintered pellets of LCMO (with $x = 0.35$) showing the influence of isotope exchange on the ferromagnetic transition temperature T_c. The measurements were carried out in a field of 50 G (field cooled) for a ^{16}O sample (solid circles), ^{18}O concentration $\approx 80\%$ (open circles), and ^{18}O samples back-exchanged with ^{16}O (open squares).

carrying out a final anneal at 1200 °C in 1 atm of pure O$_2$. This pellet was divided into two pieces and treated in 1 atm of ^{16}O or ^{18}O in a parallel processing system.[24] The pellets were gas exchanged at 950 °C (48 h), 1100 °C (48 h), and finally 1150 °C (48 h). This resulted in a pellet with an ^{18}O concentration of 82% as determined by weighing. The transition temperatures and magnetoresistances of the pellets were determined[24] using magnetic and resistivity measurements, and in the case of the ^{18}O pellet, it was found that back exchange with ^{16}O restored the original transition. The results of the magnetic measurements are shown in Fig. 1 for reference purposes. The transition temperatures are determined by extrapolating the decreasing ferromagnetic component of the magnetization to zero. For the ^{16}O sample, one obtains $T_c = 270$ K, in good agreement with other literature values. Exchange with ^{18}O causes a depression of 8.2 K in T_c (Fig. 1), which in turn yields[24] an oxygen isotope exponent of 0.26.

The Raman-scattering experiments were carried out in a quasibackscattering configuration using the 488.0- or 514.5-nm lines of an argon laser. The spectra were obtained from the as-produced faces of the pellets. The relatively weak signals were collected and dispersed in a triple spectrometer and detected with a Mepsicron imaging detector as described in detail elsewhere.[35]

Iliev *et al.*[27] also used the 514.5-nm line of an Ar ion laser to excite LMO spectra and found that the results depended critically on the incident power level used. At low power levels they found that the spectrum contained four well-defined peaks characteristic of the orthorhombic structure, but at higher power levels the peaks decreased both in number and sharpness. They attributed this rather dramatic change to the structural instability of LMO and a laser (thermally) driven structural transition to the rhombohedral phase. In contrast to this result, we have not been able to detect any dependence on the incident laser power level in

the spectra we have obtained from the doped compounds. In this regard it should be noted that the incident laser light was normally focused on the crystal using a cylindrical lens to yield an incident power density of about 10 W/cm^2. This level is considerably smaller than the smallest incident power densities ($\approx$1000 W/cm^2) used by Iliev et al.[27] Even with comparable incident power densities, however, we did not notice any dramatic changes in the spectra. This perhaps suggests that doping the pure compound (LMO) with calcium produces a more stable orthorhombic structure than that of the undoped precursor.

B. Symmetry considerations

The symmetry of the LCMO crystal structure for $0.1 < x < 0.5$ has been determined from neutron-scattering experiments[36–39] and is similar to that of the parent LMO compound[40–42] as determined by x-ray-diffraction measurements. The symmetry of the unit cell was described[36–39] in terms of an orthorhombic structure (Pnma) that resulted from small distortions of the basic cubic perovskite structure. For a calcium concentration of $x = 0.35$, Dai et al.[39] measured the orthorhombic lattice parameters and found $a = 5.455$ Å, $c = 5.470$ Å, and $b = 5.450$ ($2^{1/2}$) Å at 320 K. These results imply a value of $a_0 \approx 3.860$ Å for the lattice parameter of the basic cubic perovskite unit cell. Given that our growth conditions were similar to those used in Refs. 36 and 39, we expect that our samples will have the same structure. As a check, we have carried out x-ray-diffraction measurements on our $x = 0.35$ samples and found that the most intense Bragg peaks can be indexed onto a cubic unit cell with $a \approx 3.863$ Å. The excellent agreement with the results of Dai et al.[39] is consistent with our expectations of orthorhombic symmetry.

The crystallites in our samples are thus assumed to have a structure with orthorhombic symmetry described by the Pnma (D_{2h}^{16}) space group.[36,39] There are four molecular units (60 vibrational modes at the zone center) in the unit cell whose symmetry operations are those of the D_{2h} point group. A correlation of the site symmetries[43] with the crystal symmetry enables one to identify the irreducible representations that describe the various normal modes of vibration associated with each atomic species at the center of the Brillouin zone:

$$C_1 \; [8O(1)]: \quad 3A_g + 3B_{1g} + 3B_{2g}$$
$$+ 3B_{3g} + 3A_u + 3B_{1u} + 3B_{2u} + 3B_{3u},$$

$$C_s \; [4La(Ca) \text{ and } 4O(2)]: \quad 4A_g + 2B_{1g} + 4B_{2g}$$
$$+ 2B_{3g} + 2A_u + 4B_{1u} + 2B_{2u} + 2B_{3u},$$

$$C_i \; (4Mn): \quad 3A_u + 3B_{1u} + 3B_{2u} + 3B_{3u}.$$

The even modes are all Raman active, and thus there are a total of 24 Raman-active modes that might appear in the spectrum, but we have observed only a few of these. Unfortunately, since our spectra were obtained from pressed pellets, we cannot definitively identify the mode symmetries. In this regard, however, it is important to note that the Mn
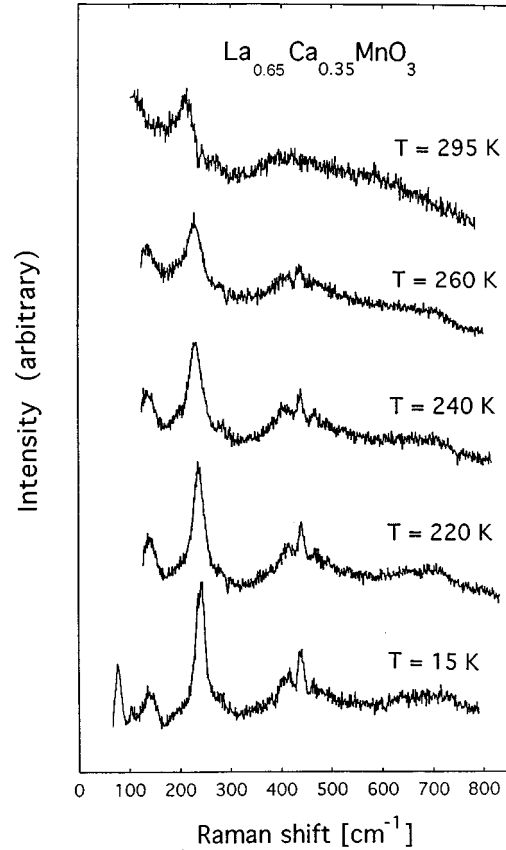

FIG. 2. Raman spectra of LCM ^{16}O ($x = 0.35$) for temperatures above and below $T_c = 272$ K.

atoms are situated at sites that are centers of inversion, and hence they must be stationary in any Raman-active or even vibration. The O(2) apical oxygens and the La (Ca) atoms are in sites with reflection symmetry (Cs), and the O(1) atoms are in C_1 sites. All the O and La atoms thus can participate in the Raman-active vibrations.

III. VIBRATIONAL SPECTRUM OF LCM ^{16}O

The low-energy ($\omega < 800$ cm^{-1}) Raman spectra of LCM ^{16}O ($x = 0.35$) are shown in Fig. 2 for a series of temperatures both above and below the transition. As shown in the figure, the vibrational modes become noticeably stronger and sharper as the temperature is lowered. In particular, the two modes with nominal frequencies of 230 and 430 cm^{-1} which are barely visible at room temperature become well defined as the temperature is reduced below about 250 K. There are five peaks that can be identified at low temperatures that occur at 70, 133, 235, 435, and 670 cm^{-1} and a broad feature at about 670 cm^{-1}. Although they were not studied in detail, spectra were also obtained from samples with $x = 0.2$ in the frequency range 200–500 cm^{-1}. These spectra were similar to the 0.35 spectra except for a frequency shift to higher energies (Table I) of the mode near 230 cm^{-1}. The number of modes and temperature dependence of the spectra shown in Fig. 2 are qualitatively similar to spectra obtained by Iliev et al.[27,28] from the orthorhombic undoped compound LaMnO$_3$ and by Podobedev et al.[29] from LSMO. The phonon frequencies for the three compounds are summarized in Table I.

TABLE I. Frequencies (in cm^{-1}) of the principal features of the spectra shown in Figs. 2 and 3 for the isotope-exchanged samples with calcium concentration $x=0.35$. Frequencies from samples with $x=0.20$ are also included, but only the O(1) mode was well defined in these spectra. The uncertainties in the frequencies are ± 2 cm^{-1} unless otherwise noted. Also included in the table (first and last rows) are data obtained from the undoped compound (Refs. 27 and 28) and a Sr-doped compound (Ref. 29).

Compound	ω_1	ω_2	ω_0 {O(1) mode}	ω_3	ω_4
$LaMnO_3$ (Ref. 28)		140	284	498	612
$La_{0.65}Ca_{0.35}Mn$ $^{16}O_3$	70	133	235	436	670 (± 5 cm^{-1})
$La_{0.65}Ca_{0.35}Mn$ $^{18}O_3$	70	133	227	415	
$La_{0.80}Ca_{0.20}Mn$ $^{16}O_3$			243	433 (± 5 cm^{-1})	
$La_{0.80}Ca_{0.20}Mn$ $^{18}O_3$			233	425 (± 5 cm^{-1})	
$La_{0.80}Sr_{0.20}Mn$ $^{16}O_3$ (Ref. 29)			232	440 ($x'y'$)	660

The spectra obtained from the LCM ^{18}O sample are similar to those for LCM ^{16}O as can be seen from a comparison of the low-temperature spectra shown in Fig. 3 for each compound. Here the higher-energy modes at 435 and 670 cm^{-1} are shifted to lower energies by about 5% in the LCM ^{18}O spectrum and can thus be attributed to vibrations of the oxygen atoms. The mode at 230 cm^{-1} is also shifted to lower energies by about 4% in the isotope-exchanged sample. Finally, there appears to be some weak ''fine structure'' around the 435-cm^{-1} feature. The origin of these weaker features is not clear, but it would be interesting to attempt to correlate these features with vibrations around the different manganese sites. The 230-cm^{-1} mode, however, appears to be the most interesting feature of the spectra shown in Fig. 2 in that its frequency is very sensitive to both temperature (Fig. 4) and Ca concentration as is demonstrated by the measurements on the 0.2 sample (Table I).

Since our spectra were obtained from polycrystalline samples, we were not able to determine the symmetries of the various modes, which would assist in identifying their origin. However, spectra have been obtained from single crystals of the undoped compound (LMO) (Refs. 27 and 28) and from LSMO,[29] which have the same structure as LCMO. In the frequency range $\omega > 200$ cm^{-1}, the spectra are qualitatively similar and thus useful information, in the form of mode identification, can be obtained from a comparison of these results with our spectra. Podobedev et al.[29] observed a mode near 220 cm^{-1} ($x=0.30$) in LSMO whose frequency increased rapidly with decreasing x and reached a value of about 280 cm^{-1} for a Sr concentration $x=0$. Iliev et al.[28] also observed an A_g mode in LMO at 284 cm^{-1} that they have assigned to the rotational soft mode on the basis of lattice dynamics calculations and comparisons with other perovskite structures. This mode involves motion of the O(1) atoms and an effective rotation of the MnO octahedra. It
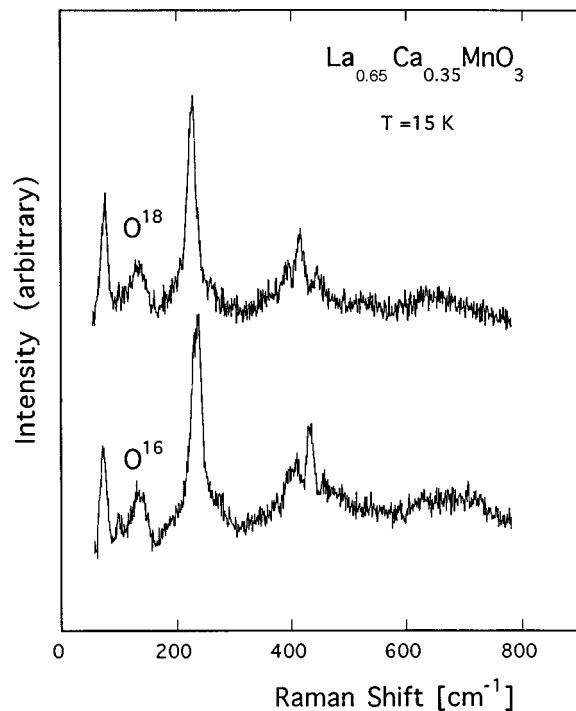

FIG. 3. Low-temperature Raman spectra of LCM ^{16}O ($x=0.35$) and LCM ^{18}O($x=0.35$).
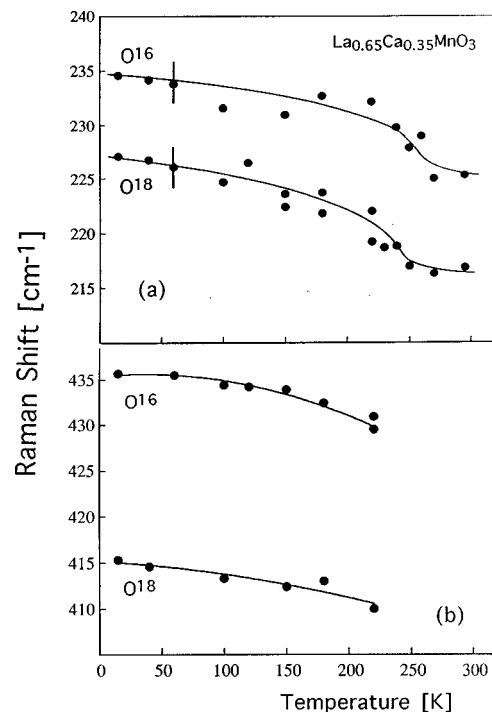
FIG. 4. Temperature dependence of the frequency of (a) the O(1) phonon in LCM ^{16}O ($x=0.35$) and LCM ^{18}O ($x=0.35$) and (b) the 430-cm^{-1} phonon in both compounds.

should thus be sensitive to structural modifications, such as JT distortion, which are modified by doping. Finally, the 230-cm^{-1} mode we observe in LCMO is in the same frequency range and exhibits a similar dependence on doping. These observations justify the assignment of a common vibrational origin to this mode in all three compounds, an assignment that is supported by the observation of an oxygen-isotope shift (Fig. 3). We will thus tentatively assume the same O(1) origin[28] for the mode and designate the 230-cm^{-1} feature and its analog in LMO and LSMO as the O(1) phonon, with frequency ω_0 and linewidth Γ_0.

IV. DOPING DEPENDENCE OF THE O(1) PHONON FREQUENCY

The above assignment does not appear to be completely consistent with observation in that the frequency is very sensitive to the Ca or Sr concentration and in fact decreases with increasing Ca concentration. It is possible that the La (Ca) atoms could be involved in the vibration, but this would imply that the frequency should increase as the lighter Ca atoms are substituted for La, which is in direct contrast to the observed behavior. The substitution of Ca has an additional indirect effect, however, in that it causes structural changes that influence the amount of distortion in the lattice. The observed frequency shifts of the O(1) phonon with doping appear to be determined by the strength of this distortion. To demonstrate this more clearly, we will use the tolerance factor[44]

$$t = \frac{\langle r_A \rangle + r_0}{\langle r_B \rangle + r_0} \qquad (1)$$

to characterize the structural modifications caused by Ca substitution. Here $\langle r_A \rangle$ is the average ionic radius of the La^{3+} (Ca^{2+}) ions and $\langle r_B \rangle$ is the average radius of the Mn^{3+} (Mn^{4+}) ions. The tolerance factor $t=1$ for the ideal perovskite structure and becomes smaller as $\langle r_A \rangle$ is reduced and the lattice becomes more distorted.[24] As $\langle r_A \rangle$ is reduced, the MnO$_6$ polyhedra adjust themselves to the smaller A atoms by rotation and tilting. This in turn leads to departures of the Mn-O-Mn angle from $180°$, which leads to a reduction of the double-exchange interaction. Sasaki et al.[44] found a relation between the bond angle and tolerance factor, and more recently others[24,45–47] have shown that the resistivity and transition temperature in the manganates are correlated with the tolerance factor. This suggests that one should also search for a correlation between the frequency of the O(1) phonon and the tolerance factor.

We have thus determined t as a function of x using the ionic radii given by Shannon.[48] In this case the appropriate radii (in angstroms) are $r(La^{3+}) = 1.36$, $r(Ca^{2+}) = 1.34$, $r(Mn^{3+}) = 0.645$, $r(Mn^{4+}) = 0.53$, $r(O^{2-}) = 1.40$, and $r(Sr^{2+}) = 1.44$. For the stoichiometric oxygen formula content of 3.0, the Mn^{4+} content is given by x. The results are plotted in Fig. 5 where it can be seen that the addition of Ca or Sr to LMO results in an approximately linear increase of t with increasing x. Thus, although the addition of Ca reduces $\langle r_A \rangle$, this is offset by the greater reduction in $\langle r_B \rangle$ caused by the corresponding increase in the Mn^{4+} concentration. The frequencies of the O(1) mode for LSMO from Ref. 29 and
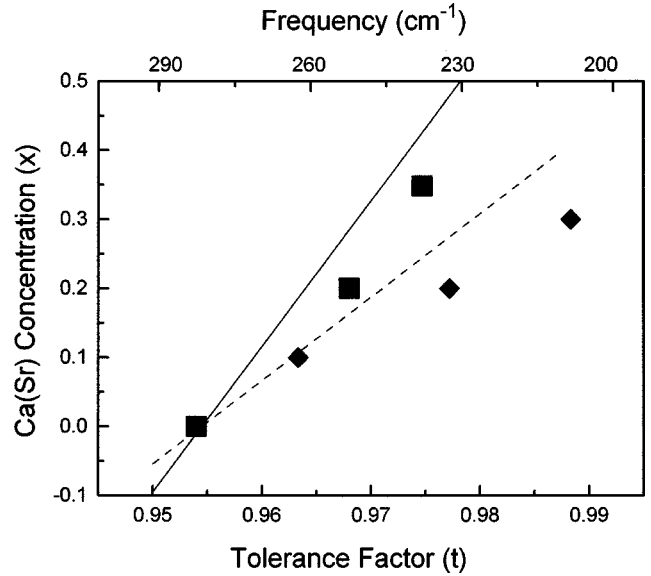

FIG. 5. Plot of the tolerance factor t as a function of Ca concentration in LCM ^{16}O (solid line) and Sr concentration in LSM ^{16}O (dashed line). The measured frequencies of the O(1) phonon in LCM ^{16}O are shown as solid squares and superimposed on the plot. Also, frequencies obtained from Ref. 29 for LSM ^{16}O are shown in the plot for three different values of x (diamonds). Finally, the large square near 280 cm^{-1} represents the results for LMO (Refs. 28 and 29).

for LCMO from Table I are superimposed on the same plot. Although the amount of data is limited, there appears to be a good correlation between t and the O(1) phonon frequency ω_0. Thus we will attribute variations in ω_0 with x to the structural modifications induced by Ca or Sr doping. It is interesting to note (Fig. 5) that ω_0 increases as the Mn^{4+} concentration decreases.

V. TEMPERATURE DEPENDENCE OF THE O(1) PHONON FREQUENCY

As remarked above, the frequency of the O(1) phonon (ω_0) hardens significantly (Fig. 4) as the temperature is reduced from a value just above T_c to about 15 K. The temperature dependence of the 435-cm^{-1} mode is shown in Fig. 4(b) for comparison purposes. In this case the mode is observed only in spectra obtained below T_c and it exhibits a more typical anharmonic temperature dependence[49] in that there is very little variation below 100 K.

As is evident from Fig. 4, ω_0 undergoes a rather abrupt increase in frequency (≈ 4 cm^{-1}) as the temperature is lowered through the transition at T_c. Furthermore, as the temperature is lowered from about 250 to 15 K, the frequency of the mode continues to increase at a rate that appears to be in excess of normal anharmonic variations.[49] At first glance one might assume that the frequency shift at T_c should be attributed to a structural change that occurs as the sample goes from the PI phase to the FM phase. However, it is expected that such a structural change should result in the decrease of the number of Jahn-Teller sites[9–16] and hence a more ordered structure at lower temperature. The phonon frequency should then decrease to be consistent with the behavior shown in Fig. 5. Since ω_0 actually increases at T_c, it is clear that
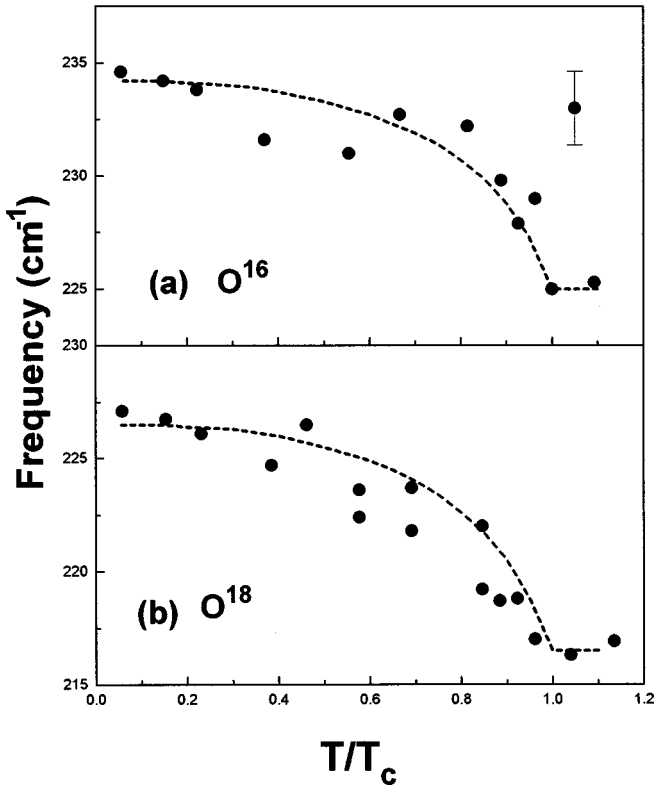
FIG. 6. Comparison of frequencies obtained from Eq. (3) in text (dashed line) with the measured frequencies (solid circles) in (a) LCM ^{16}O ($x = 0.35$) and (b) LCM ^{18}O ($x = 0.35$).

additional mechanisms must be influential in determining the temperature dependence of the O(1) phonon frequency. In this regard Millis et al.[9,10] have suggested that a strong electron-phonon interaction in combination with the double-exchange mechanism is required to explain the properties of the CMR compounds. This scenario has been investigated theoretically by Lee and Min[33] who found

$$\hat{\omega}_q^2 = \omega_q^2 - 2\omega_q |M_q|^2 \frac{1}{\gamma(T)} \sum_{\mathbf{k}} \frac{n_{\mathbf{k}} - n_{\mathbf{k}+\mathbf{q}}}{t_{\mathbf{k}+\mathbf{q}} - t_{\mathbf{k}}}, \qquad (2)$$

where $\hat{\omega}_q$ is the renormalized frequency, M_q is the electron-phonon coupling constant, and $n_{\mathbf{k}}$ and $t_{\mathbf{k}}$ are the number operator and transfer integral, respectively, $t[\gamma(T)] = t\langle \cos(\theta_{ij}/2) \rangle$ is the "double exchange" bandwidth, where t is the hopping parameter. θ_{ij} is the angle between the spins on sites i and j and the brackets indicate a mean-field average over all sites. For the purposes of comparison with the data, Eq. (2) can be rewritten as

$$\hat{\omega}_q \approx \omega_q \sqrt{1 - \beta/\gamma(T)}, \qquad (3)$$

where β is approximately independent of temperature.[22]

To calculate the renormalized frequency for comparison with experiment, we have obtained values for the "double-exchange" parameter $\gamma(T)$ in the mean-field approximation as described by Kubo and Ohata.[50] A comparison with the data is shown in Fig. 6 where we have plotted $\hat{\omega}_q$ versus T/T_c with $\beta = 0.147$ for LCM ^{16}O and $\beta = 0.164$ for LCM ^{18}O. As is evident from the figure, the agreement be-

tween model and experiment is quite good in that the model captures the rather abrupt changes that occur near T_c and reproduces the overall dependence on T in a satisfactory manner. The fact that bandwidth changes appear to determine the increase in ω_0 at T_c, in conjunction with the expectation of increased order below T_c and the consequent implications of Fig. 5, suggests that there are no significant structural modifications at T_c.

For the purpose of the fits shown in Fig. 6 $\gamma(T)$ is assumed to be the same for both compounds and this leads to a 10% increase in the value of β for LCM ^{18}O. However, one can see from Eqs. (2) and (3) that $\beta \propto |M_q|^2/\omega_q$, and since $|M_q|^2 \propto \omega_q$, the fitting parameter β should be independent of isotope exchange. One should note, however, that the increase in the fitting parameters occurs because $\{\hat{\omega}_q(15\,\text{K}) - \hat{\omega}_q(T_c)\}$ is about 1 cm^{-1} or 10% larger for LCM ^{18}O than it is for LCM ^{16}O. Since this difference is comparable with the experimental uncertainty in the individual points, it is difficult to make any definitive statements concerning the different magnitudes of $\gamma(T)$ that are implied by the fitting procedure. However, it is interesting to speculate on the consequences of using the polaron bandwidth $W \propto \gamma(T)\gamma_p(T)$, where $\gamma_p(T) = \exp\{-\Sigma |u_q|^2(n_q + 1/2)\}$, in Eq. (2) for the fitting process. Here $|u_q| \propto |M_q/\omega_q| \propto (\omega_q)^{-1/2}$, and thus γ_p is sensitive to isotope exchange. In fact, Shengelaya et al.[20] have found that oxygen isotope exchange leads to a 10% reduction in the bandwidth W, and thus the use of W in Eq. (2) for the fitting process would thus lead to a constant β. In other words, the temperature dependence would still be determined primarily[33] by $\gamma(T)$, but the magnitude of the bandwidth would depend on the atomic mass through $\gamma_p(T)$. We must emphasize, however, that the present data are not precise enough to allow us to draw any firm conclusions regarding the role of the polaron bandwidth in determining the phonon frequencies.

Our results can also be compared to the extended x-ray-absorption fine-structure (EXAFS) measurements of Booth et al.[15] who have shown that the Mn-O bond lengths are essentially independent of temperature and, in particular, are rather insensitive to the PI-to-FM transition. On the other hand, they found that the Debye-Waller broadening parameter σ^2 for the Mn-O bond decreases significantly near T_c, which is consistent with an increase in the Mn-O spring constant and hence the O(1) frequency ω_0.

VI. TEMPERATURE DEPENDENCE OF Γ_0

The linewidth Γ_0 of the O(1) phonon has been determined from Lorentzian fits to both the LCM ^{16}O and LCM ^{18}O spectra at various temperatures. In determining the linewidths a linear background term was added to the Lorentzian profile to obtain good fits to the measured profiles (examples are shown in Fig. 7). The values for Γ_0 obtained from these fits are plotted as a function of temperature in Fig. 8. Again, the transition temperatures are marked by a clearly observable change in the temperature dependence of Γ_0 at T_c. At the critical temperature the linewidth Γ_0 changes abruptly in both compounds and then decreases rapidly in the region $230\,\text{K} < T < 270\,\text{K}$. The change in Γ_0 that occurs near T_c could be associated with a structural change in the material that leads to increased order below T_c. However, as dis-

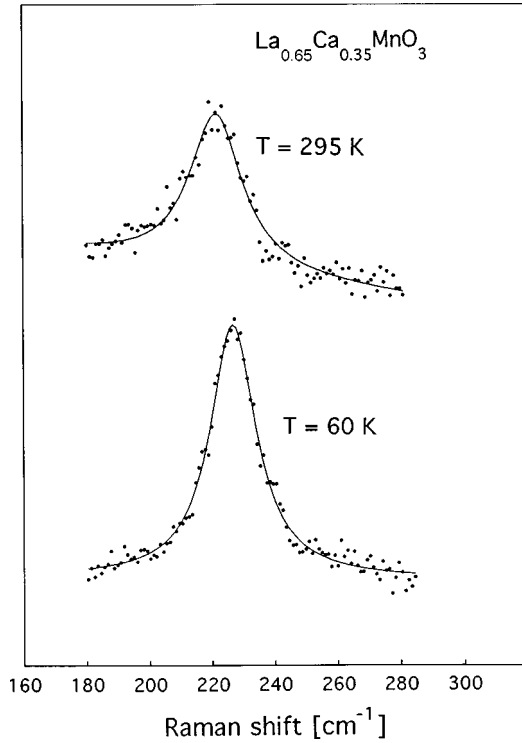FIG. 7. Examples of Lorentzian fits to the measured line shapes of the O(1) phonon in LCM ^{16}O ($x=0.35$) for temperatures above and below T_c.

cussed above, such a structural change should lead to a decrease in ω_O (Fig. 5). This is certainly not consistent with the observed increase (Fig. 4) in the mode frequency at T_c. We thus conclude that other broadening mechanisms are more important in this temperature range.

To investigate the line broadening in more detail, we can again compare our results to the calculations of Lee and Min.[33] In their model the phonon linewidth is given by

$$\Gamma_q = 2\omega_q |M_q|^2 \frac{\pi \mathcal{J}(E_F)}{2v_F q} \frac{1}{\gamma(T)^2} = \frac{C(q)}{\gamma(T)^2}, \qquad (4)$$
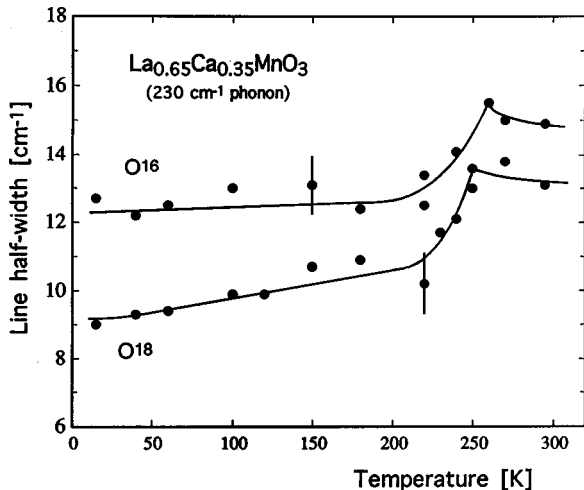

FIG. 8. Temperature dependence of the half width at half maximum (HWHM) of the O(1) phonon for LCM ^{16}O ($x=0.35$) and LCM ^{18}O ($x=0.35$).
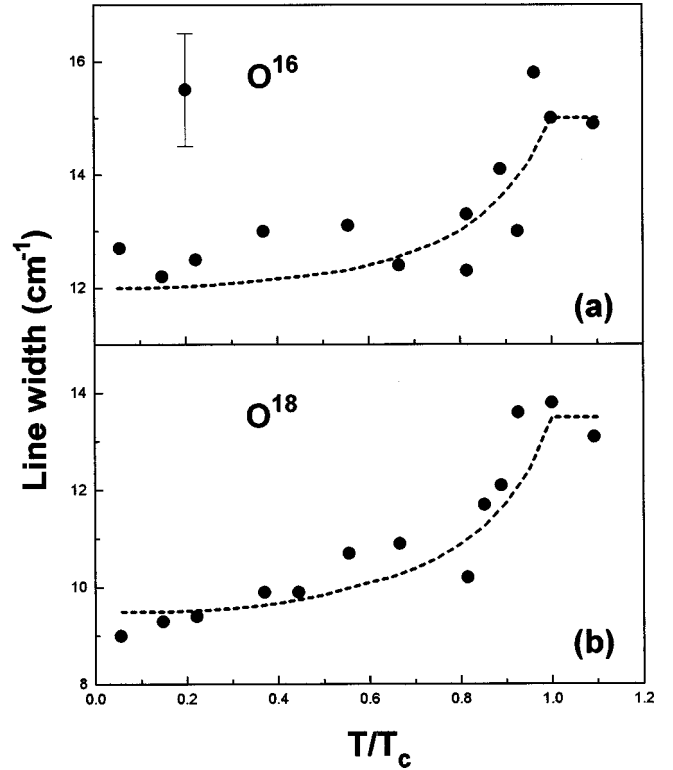

FIG. 9. Comparison of linewidths Γ_0 obtained from Eq. (5) in text (dashed lines) with the measured values (solid circles) for (a) LCM ^{16}O ($x=0.35$) and (b) LCM ^{18}O ($x=0.35$).

where $\mathcal{J}(E_F)$ and v_F are the density of states and velocity at the Fermi surface. Here we assume that the temperature dependence of Γ_q is determined primarily by $\gamma(T)$. To compare with experiment we can divide Γ_0 into two parts, a temperature-independent part Γ_1 and a temperature-dependent part Γ_q:

$$\Gamma_0 = \Gamma_1 + \Gamma_q = \Gamma_1 + C/\{\gamma(T)\}^2. \qquad (5)$$

The linewidths obtained from Eq. (5) with $\Gamma_1 = 8.14(4.36)$ and $C = 2.47(3.29)$ for LCM ^{16}O (LCM ^{18}O) are compared with the experimental results in Fig. 9. Here $\gamma(T)$ was again determined following Ref. 50 and is again assumed to be the same for both compounds. As can be seen from the figure, the agreement between model and experiment is very good in that the major features of the data are reproduced. That is, the rather abrupt change in Γ_0 near T_c and the continuing decrease as T is reduced further are nicely captured by the model. The temperature-independent component that arises from the fits may be associated with structural distortions that remain approximately constant as the temperature is lowered, consistent with the absence of structural modifications at T_c.

We can also note that it is very clear from the spectra that the measured linewidths in LCM ^{18}O are consistently smaller than those in the LCM ^{16}O spectra. This observation appears to be consistent with the predictions of Lee and Min[33] since from Eq. (4) we can see that $\Gamma_q \propto C \propto |M_q|^2 \omega_q \propto \omega_q^2$. Oxygen isotope exchange should thus lead to a reduction in Γ_q of up to $\{M(18) - M(16)\}/M(16)$ or about 12.5%. As is evident from Fig. 8, this prediction is in reasonable agreement with

the measured difference of about 1.5 cm^{-1} at room temperature. We can also note (Fig. 9) that the change in linewidth with temperature, $\Gamma_q(T_c) - \Gamma_q(15 \text{ K})$, is about 1 cm^{-1} (25%) greater for LCM ^{18}O than it is for LCM ^{16}O. With fixed $\gamma(T)$, the fit to the ^{18}O data thus leads to a corresponding increase in the constant C. This result appears to be in conflict with the isotope-induced change in linewidth which requires a reduction in C for LCM ^{18}O. However, one must again note that the difference of 1 cm^{-1} between the temperature variations for the ^{16}O and ^{18}O linewidths is comparable to the experimental uncertainty involved in the individual linewidth measurements, and thus it is difficult to draw definitive conclusions. It is again interesting to note, however, that if the polaron bandwidth was used in the fitting equation (5), one would be able to use the smaller value of C that is required to obtain agreement between Eq. (4) and the smaller linewidths that are observed in LCM ^{18}O (Fig. 9).

It is somewhat surprising that a Lorentzian profile provides an excellent fit to the measured line shape (Fig. 7) for all $T < T_c$. In other words, there is no hint of a Fano profile asymmetry[33] in the phonon line shapes, at any temperature, that would occur because of coupling to an electronic continuum as is observed[51] in some other strongly correlated electron systems such as YBa$_2$Cu$_3$O$_7$. Thus the phonon line shape does not provide any indication of the increase in carrier concentration that presumably occurs below T_c. It might be possible that the ''free'' electron density might remain small and the typical Fano effect is not observable. Since this possibility is at variance with transport measurements,[24,25] we do not have a satisfactory explanation for the absence of an observeable Fano interaction.

VII. INFLUENCE OF OXYGEN ISOTOPE EXCHANGE

The effects of isotope exchange on the Raman spectrum are shown in Fig. 3 where the low-temperature spectra of LCM ^{16}O and LCM ^{18}O are directly compared. From the figure it is evident that some of the modes are shifted to lower frequencies, indicating the contribution of oxygen vibrations to that particular mode. The O(1) mode is shifted by about 4%, which suggests that the crystal is not completely exchanged or that both O and La atoms are involved in the vibration. In this regard the samples were found[24,25] to be 82% exchanged from weight measurements. The 435-cm^{-1} mode is shifted by about 5%, which is about the maximum (5.7%) obtainable by oxygen isotope exchange. This suggests that only oxygen atoms are involved in the vibration, consistent with the relatively large frequency of the mode. Similarly, one would expect that any higher-frequency modes arise from vibrations of the oxygen atoms. As noted above, however, the exchange of isotope might also have an indirect effect on the frequency because of the reduction in the effective bandwidth caused by the heavier isotope. If one uses Eq. (2) to estimate the possible effect of this reduction in bandwidth, one finds that the phonon frequency is reduced by about 2% due to a 10% change in bandwidth. The effect is thus non-negligible relative to the mass-induced shift and could complicate the determination of the degree of isotope exchange from phonon measurements.

In the case of the linewidth measurements, we have noted that the measured values of Γ_0 for LCM ^{18}O are noticeably smaller than those obtained from the LCM ^{16}O spectra. We have also noted that this difference can be attributed to the smaller electron-phonon coupling constant in LCM ^{18}O. This is consistent with the observation that the spectra obtained from LCM ^{18}O are qualitatively superior in terms of clarity and background than those obtained from LCM ^{16}O. However, there is also a significant constant contribution Γ_1 [Eq. (5)] involved in the linewidth fits. Thus it is reasonable to assume that the phonon linewidth is influenced by several factors. For example, one might speculate that spin-phonon interactions play a role and that the reduced J (Ref. 20) in the LCM ^{18}O compounds results in a reduced spin-phonon interaction.[52] A quantitative estimate of such a contribution will require a much more detailed comparison with the results of magnetic measurements.[53]

VIII. CONCLUSIONS

The Raman spectra of the CMR compounds LCM ^{16}O ($T_c = 270$ K) and LCM ^{18}O ($T_c = 262$ K) have been measured as a function of temperature. The vibrational spectrum is weak at 300 K, but increases in strength as the temperature is reduced to 15 K. This behavior and the observed mode structure are similar to the spectra observed for the related compounds LMO (Refs. 27 and 28) and LSMO.[29] The most interesting feature in the LCMO spectra is a mode that arises from vibrations of the O(1) atoms. The frequency ω_0 of this mode hardens significantly when the Ca concentration in LCMO (or the Sr concentration in LSMO) is reduced. We have shown that the doping dependence of the phonon frequency is correlated with the distortion in the lattice by using the tolerance factor to characterize the distortion in compounds with different dopings. This correlation suggests that the phonon frequency decreases as the distortion in the lattice decreases or as the Mn-O-Mn bond angle becomes larger and approaches 180°.

The O(1) phonon frequency hardens noticeably as the sample is cooled through T_c and continues to harden as the sample is cooled to 15 K. This dependence of ω_0 on temperature is qualitatively reproduced by a model[33] that incorporates a double-exchange mechanism in the presence of an electron-phonon interaction. In this case the temperature dependence of the phonon is determined by the temperature dependence of the effective ''double-exchange'' bandwidth $\gamma(T)$. The observed abrupt increase in ω_0 near T_c (Fig. 5) is nicely described by the predicted[33] variation in $\gamma(T)$, which implies that there are no significant structural changes at the transition. These features are consistent with EXAFS measurements[15] which imply an increase in phonon frequency as the sample is cooled through T_c without any significant changes in the Mn-O bond angles at the transition.

The linewidth of the O(1) phonon is found to decrease significantly just below T_c, and continues to decrease as T is reduced further, in both LCM ^{18}O and LCM ^{16}O. The observed dependence of Γ_0 on temperature is also described very well by assuming that it is determined by the variation of γ with T. We have also found that the linewidth of the O(1) phonon is smaller in LCM ^{18}O than it is in LCM ^{16}O. This decrease is predicted by the model of Lee and Min[33] and can be attributed to the fact that the electron-phonon coupling constant is smaller in LCM ^{18}O than it is in

LCM ^{16}O. The variation of the constants used to obtain the frequency (Fig. 6) and linewidth (Fig. 9) fits for both LCM ^{18}O and LCM ^{16}O have led us to speculate that it might be more appropriate to use the full polaron bandwidth W in Eqs. (2) and (4). However, further work will be required to validate this speculation. Finally, the measured phonon line shapes do not provide any evidence of a coupling between phonons and a free-electron continuum in that they are well described by simple Lorentzian profiles at all temperatures.

[1] G. H. Jonker and J. H. van Santen, Physica (Amsterdam) **16**, 337 (1950).

[2] E. Wollan and W. C. Koehler, Phys. Rev. **100**, 545 (1955).

[3] J. Volger, Physica (Amsterdam) **20**, 49 (1954).

[4] C. Zener, Phys. Rev. **82**, 403 (1951).

[5] P. W. Anderson and H. Hasegawa, Phys. Rev. **100**, 675 (1955).

[6] P. G. de Gennes, Phys. Rev. **118**, 141 (1960).

[7] P. Schiffer, A. P. Ramirez, W. Bao, and S.-W. Cheong, Phys. Rev. Lett. **75**, 3336 (1995).

[8] S. Jin, T. H. Tiefel, M. McCormack, R. A. Fastnacht, R. Ramesh, and L. H. Chen, Science **264**, 413 (1994).

[9] A. J. Millis, P. B. Littlewood, and B. I. Shraiman, Phys. Rev. Lett. **74**, 5144 (1995).

[10] A. J. Millis, R. Mueller, and B. I. Shraiman, Phys. Rev. B **54**, 5389 (1996); **54**, 5405 (1996).

[11] H. Roder, J. Zang, and A. R. Bishop, Phys. Rev. Lett. **76**, 1356 (1996); Phys. Rev. B **53**, R8840 (1996).

[12] J. L. Garcia-Munoz, M. Suaaidi, J. Fontcuberta, and J. Rodriguez-Carvajal, Phys. Rev. B **55**, 34 (1997).

[13] D. Louca, T. Egami, E. L. Brosha, H. Roder, and A. R. Bishop, Phys. Rev. B **56**, R8475 (1997).

[14] S. J. L. Billinge, R. G. DiFrancesco, G. H. Kwei, J. J. Neumeier, and J. D. Thompson, Phys. Rev. Lett. **77**, 715 (1996).

[15] C. H. Booth, F. Bridges, G. J. Snyder, and T. H. Geballe, Phys. Rev. B **54**, R15 606 (1996).

[16] C. Booth, F. Bridges, G. H. Kwei, J. M. Lawrence, A. L. Cornelius, and J. L. Neumeier, Phys. Rev. Lett. **80**, 853 (1998).

[17] P. Dai, J. Zhang, H. A. Mook, S.-H. Liou, P. A. Dowben, and E. W. Plummer, Phys. Rev. B **54**, R3694 (1996).

[18] T. A. Tyson, J. Mustre de Leon, S. D. Conradson, A. R. Bishop, J. J. Neumeier, H. Roder, and J. Zang, Phys. Rev. B **53**, 13 985 (1996).

[19] S. B. Oseroff, M. Torikachvili, J. Singley, S. Ali, S.-W. Cheong, and S. Schultz, Phys. Rev. B **53**, 6521 (1996).

[20] A. Shengelaya, G.-m. Zhao, H. Keller, and K. A. Muller, Phys. Rev. Lett. **77**, 5296 (1996).

[21] R. H. Heffner, L. P. Le, M. F. Hundley, J. J. Neumeier, G. M. Luke, K. Kojima, B. Nachumi, Y. J. Uemura, D. E. McLaughlin, and S.-W. Cheong, Phys. Rev. Lett. **77**, 1869 (1996).

[22] K. H. Kim, J. Y. Gu, H. S. Choi, G. W. Park, and T. W. Noh, Phys. Rev. Lett. **77**, 1877 (1996).

[23] Guo-meng, Zhao, K. Conder, H. Keller, and K. A. Muller, Nature (London) **381**, 676 (1996).

[24] J. P. Franck, I. Isaac, W. Chen, J. Chrzanowski, and J. C. Irwin, Phys. Rev. B **58**, 5189 (1998); J. Phys. Chem. Solids **59**, 2199 (1998).

[25] I. Isaac and J. P. Franck, Phys. Rev. B **57**, R5602 (1998); J. Phys. Chem. Solids **59**, 2208 (1998).

[26] W. Pickett, Nature (London) **381**, 651 (1996).

[27] M. N. Iliev, M. V. Abrashev, H. G. Lee, V. N. Popov, Y. Y. Sun, C. Thomsen, R. L. Meng, and C. W. Chu, J. Phys. Chem. Solids **59**, 1982 (1998).

[28] M. N. Iliev, M. B. Abreshev, H.-G. Lee, V. N. Popov, Y. Y. Sun, C. Thomsen, R. L. Meng, and C. W. Chu, Phys. Rev. B **57**, 2872 (1998).

[29] V. B. Podobedov, A. Weber, D. B. Romero, J. P. Rice, and H. D. Drew, Solid State Commun. **105**, 589 (1998); in *Science and Technology of Magnetic Oxides*, edited by M. Hundley, J. Nickel, R. Ramesh, and Y. Tokura, MRS Symposia Proceedings No. 494 (Materials Research Society, Pittsburgh, 1998), p. 329.

[30] R. Gupta, A. K. Sood, R. Mahesh, and C. N. R. Rao, Phys. Rev. B **54**, 14 899 (1996).

[31] G. F. Strouse, S. Cumberland, H. N. Bordallo, and D. Argyriou, Bull. Am. Phys. Soc. **43**, 163 (1998); (unpublished).

[32] Y. Okimoto, T. Katsufuji, T. Ishikawa, A. Urushibara, T. Arima, and Y. Tokura, Phys. Rev. Lett. **75**, 109 (1995).

[33] J. D. Lee and B. I. Min, Phys. Rev. B **55**, 12 454 (1997).

[34] M. V. Klein, in *Light Scattering in Solids*, edited by M. Cardona (Springer, Heidelberg, 1969), p. 147.

[35] W. G. McMullan, Ph.D. thesis, Simon Fraser University, 1988.

[36] P. G. Radaelli, D. E. Cox, M. Marezio, S.-W. Cheong, P. E. Schiffer, and A. P. Ramirez, Phys. Rev. Lett. **75**, 4488 (1995).

[37] P. G. Radaelli, D. E. Cox, M. Marezio, and S.-W. Cheong, Phys. Rev. B **55**, 3015 (1997).

[38] P. Dai, J. Zhang, H. A. Mook, S.-H. Liou, P. A. Dowben, and E. W. Plummer, Solid State Commun. **100**, 865 (1996).

[39] P. Dai, J. Zhang, H. A. Mook, S.-H. Liou, P. A. Dowben, and E. W. Plummer, Phys. Rev. B **54**, R3694 (1996).

[40] M. A. Gilleo, Acta Crystallogr. **10**, 161 (1957).

[41] J. B. A. A. Elemens, B. van Laar, K. R. van der Veen, and B. O. Loopstra, J. Solid State Chem. **3**, 238 (1971).

[42] P. Norby, I. G. Krogh Andersen, E. Krogh Andersen, and N. H. Andersen, J. Solid State Chem. **119**, 191 (1995).

[43] W. G. Fateley, F. R. Dollish, N. T. McDevitt, and F. F. Bentley, *Infrared and Raman Selection Rules for Molecular and Lattice Vibrations* (Wiley-Interscience, Toronto, 1972).

[44] S. Sasaki, C. T. Prewitt, J. D. Bass, and W. A. Schulze, Acta Crystallogr., Sect. C: Cryst. Struct. Commun. **43**, 1668 (1987).

[45] H. Y. Hwang, T. T. M. Palstra, S.-W. Cheong, and B. Batlogg, Phys. Rev. B **52**, 15 046 (1995).

[46] J. J. Neumeier, M. F. Hundley, J. D. Thompson, and R. H. Heffner, Phys. Rev. B **52**, R7006 (1995).

[47] J. Fontcuberta, B. Martinez, A. Seffar, S. Pinol, J. L. Garcia-Munoz, and X. Obradors, Phys. Rev. Lett. **76**, 1122 (1996).

[48] R. D. Shannon, Acta Crystallogr., Sect. A: Cryst. Phys., Diffr.,

Theor. Gen. Crystallogr. **32**, 751 (1976).

[49] J. Menendez and M. Cardona, Phys. Rev. B **29**, 2051 (1984).

[50] K. Kubo and N. Ohata, J. Phys. Soc. Jpn. **33**, 21 (1972).

[51] E. Altendorf, X. K. Chen, J. C. Irwin, R. Liang, and W. N. Hardy, Phys. Rev. B **47**, 8140 (1993).

[52] X. K. Chen, J. C. Irwin, and J. P. Franck, Phys. Rev. B **52**, R13 130 (1995).

[53] C. N. R. Rao and A. K. Cheetham, Adv. Mater. **9**, 1009 (1997).